Optical Materials 117 (2021) 111138

Contents lists available at ScienceDirect

Optical Materials

journal homepage: www.elsevier.com/locate/optmat

Research Article

Graphene oxide deposition on neodymium doped zinc borotellurite glass surface: Optical and polarizability study for future fiber optics

Y. Azlina [a], M.N. Azlan [a,*], S.S. Hajer [b], M.K. Halimah [c], A.B. Suriani [a], S.A. Umar [d], R. Hisam [e], M. H.M. Zaid [c], S.M. Iskandar [f], B.K. Kenzhaliyev [g], A.V. Nitsenko [g], N.N. Yusof [h], Boukhris Imed [i,j]

[a] Physics Department, Faculty of Science and Mathematics, University Pendidikan Sultan Idris, 35900, Tanjong Malim, Perak, Malaysia
[b] Physics Department, Faculty of Science, Elmergib University, Port Street Al Khums, 40414, Elmergib, Libya
[c] Department of Physics, Faculty of Science, Universiti Putra Malaysia, 43400, Serdang, Selangor, Malaysia
[d] Department of Physics, Faculty of Science, Federal University Lafia, Lafia, Nasarawa State, Nigeria
[e] Faculty of Applied Sciences, Universiti Teknologi MARA, 40450, Shah Alam, Selangor, Malaysia
[f] School of Physics, Universiti Sains Malaysia, 11800, USM, Penang, Malaysia
[g] Institute of Metallurgy and Ore Beneficiation, Satbayev University, Almaty, Kazakhstan
[h] Physics Department, AOMRG & Laser Centre, Faculty of Science, Universiti Teknologi Malaysia, 81310, Johor Bahru, Johor, Malaysia
[i] Department of Physics, Faculty of Science, King Khalid University, P.O. Box 9004, Abha, Saudi Arabia
[j] Université de Sfax, Faculté des Sciences de Sfax, Département de Physique, Laboratoire des matériaux composites céramiques et polymères (LaMaCoP) Faculté des sciences de Sfax BP 805, Sfax 3000, Tunisie

ARTICLE INFO

Keywords:
Optical bandgap
Refractive index
Oxide ion polarizability

ABSTRACT

Neodymium oxide doped tellurite-based glass has been widely documented for potential uses in optoelectronics, but graphene oxide (GO)-coated tellurite-based glass has rarely been reported. In this work, we compare two sets of glass series which were GO-coated and uncoated tellurite-based glass series denoted as ZBTNd-GO and ZBTNd, respectively. The two sets of glasses were fabricated via melt-quenched process. A set of glass was coated with GO using low-cost spray coating method. The structural and morphological properties of the glass samples were investigated to confirm the type of structure in glass and formation of graphene oxide on glass surface. The X-ray diffraction (XRD) pattern confirmed the amorphous structural arrangement in both sets of glass series. The morphological study proved the existence of GO layers on top of the ZBTNd-GO surface. The optical bandgap energy of ZBTNd-GO glass was found in the range of 3.253 eV–3.381 eV which was higher than ZBTNd glass. Meanwhile, the refractive index of ZBTNd-GO glass varies from 2.301 to 2.332 which was higher than ZBTNd glass due to the presence of functionalized oxygenated groups in GO structure. The oxide ion polarizability of ZBTNd-GO glass was found decreased due to the shift of optical band gap when coated with GO. This work offers a new form of glass that could be used as a new strategy to upgrade the current photonic materials.

1. Introduction

Graphene oxide (GO) is oxidized from a graphene derivative that can be described as a carbon-based substance composed primarily of an abundant content of oxygen-containing functionality groups found at the edges of GO structures [1,2]. The excellent properties in GO have an extraordinary interest to be included in the optoelectronics application [3,4], super-capacitors [5,6], or as an energy charge storage like GO-based lithium ion battery [7], respectively as well as suitable to be applied in the enhancement of sensing [8] and solar cells [9] applications.

In particular, the widening of band gap energy in GO structures which due to the pristine graphene through the transformation from sp^2 to sp^3 hybrid via an oxidation process, can be considered to be beneficial for enhancing the optical properties in the glass materials [10,11]. The tuning of GO band gap energy implies, in particular, the presence of higher functional groups of oxygen, which can be correlated with the effect of oxidation in GO structures [12]. The integration of graphene oxide and tellurite glass is therefore a way to further enhance the optical properties of the glass network system, as the inclusion of GO itself would perform as an ideal candidate for the production of excellent glass coatings.

* Corresponding author.
E-mail address: azlanmn@fsmt.upsi.edu.my (M.N. Azlan).

https://doi.org/10.1016/j.optmat.2021.111138
Received 22 December 2020; Received in revised form 13 April 2021; Accepted 27 April 2021
Available online 13 May 2021

Tellurite glasses provide scientific and future interest due to their physical properties, including outstanding compatibility with rare-earth, excellent optical tuning and stable glass formation [13,14]. It is therefore anticipated that the tellurite-based glass system, with the addition of GO, may enhance the optical properties that are useful for fiber optics. Neodymium ions are often chosen due to their suitability for glass-forming and high optical properties for optical sensors and laser technology with a significant potential [15,16]. In comparison, neodymium ions have special properties with a 4-level laser emission of about 1 mm, which is higher than other rare-earth ions [17].

Graphene coated-glass fibers have been extensively investigated due to their excellent optical applications especially in optical sensors, optoelectronics devices, and light-weight electromagnetic shielding. Polymer based fibers such as polyaniline and polypyrrole have several disadvantageous like expensive to produce, low performance, and difficult to fabricate. However, glass fibers have been widely commercialized due to the low-cost production and excellent optical properties. Coating the glass fibers with graphene oxide has been proved to be an excellent strategy to improve the performance of glass fibers.

Apart from the utilization of GO-based materials for advanced surface coatings, however, previous research in this area is very limited. In this work, we aim to improve the optical properties of glass materials by depositing GO on the glass surface and at the same time, this novel research may significantly achieve an interesting result, mainly for the fiber optics technology.

2. Materials and methods

2.1. Fabrication of glass

The sets of glasses named as ZBTNd-GO and ZBTNd were fabricated via melt-quenching technique. The compositions of the sets of glasses are as follows:

ZBTNd-GO/ZBTNd: $\{[(TeO_2)_{0.70}(B_2O_3)_{0.30}]_{0.70}(ZnO)_{0.30}\}_{1-y}(Nd_2O_3)_y$

$y = 0.005, 0.01, 0.02, 0.03, 0.04, 0.05$ mol%

The high purity of raw materials consists of Tellurium (IV) Oxide, TeO_2 (Alfa Aesar, 99.99%), Boron Oxide, B_2O_3 (Alfa Aesar, 98.50%), Zinc Oxide, ZnO (Alfa Aesar, 99.99%), and Neodymium (III) Oxide, Nd_2O_3 (Alfa Aesar, 99.99%). All the chemical powders were weighed using an electrical balance in accordance of calculated compositions with an accuracy of ±0.0001 g.

The weighed chemical powder was then placed into a platinum crucible and stirred for 30 min in order to obtain a completely homogeneous mixture. The platinum crucible containing raw materials was placed to the first furnace for 400 °C for an hour to undergo the pre-heating process probably to remove the water content or moisture contained in the mixture. Next, the mixture was melted with a high temperature of electrical furnace at 900 °C for 2 h certainly to obtain the good performance of transparent glass and having the low tendency of fragility in glass materials.

The molten chemical powder was poured instantly into a cylindrical stainless steel mould that had been pre-heated at 400 °C about an hour earlier to avoid the glass cracking which could result from the thermal shock and the melt was immediately annealed at 400 °C for an hour to release the thermal stress or strain and get rid of the air bubbles which might exist in glass materials. The fabricated glass samples were allowed to cool down at room temperature for 5 h before being polished on both sides using the different types of sandpaper to attain the highly flat, shiny, and smooth on glass samples surface for further optical and structural characterization in the glass materials.

2.2. Extraction and deposition of graphene oxide on the ZBTNd glass surface

The synthesis of GO commonly used graphite electrodes based on the chemical approach via an electrochemical exfoliation technique. The graphite rods were attached to a direct current (DC) power supply as the function of an anode and cathode electrodes. The electrodes was immersed into the dissolved electrolyte solution. Interestingly, a commercially anionic surfactant known as the sodium dodecyl sulphate (SDS) was added into the de-ionized (DI) water to prepare the electrolyte solution due to that surfactant can assist to promote the stabilization of graphene sheets occurred during exfoliation process [18]. In addition, the presence of a surfactant might inhibit the formation of aggregation structures. The resulting GO materials was deposited on the ZBTNd surface via simple spray coating method to carry out the analysis on the optical and structural glass properties, as summarized in Fig. 1.

3. Results and discussion

3.1. Scanning electron microscopy (SEM) analysis

Morphological analysis of ZBTNd-GO glass surface was performed using scanning electron microscopy (SEM), as depicted in Fig. 2 (a) and (b). The deposition of GO was done to upgrade the optical performance of the current tellurite-based glass. The agglomeration of graphene oxide was revealed as depicted in Fig. 2 (a) and (b) due to a certain amount of surfactant which attempts to optimize the exfoliated GO layers during the electrochemical process [19]. In addition, the GO layers include an excess of oxygen functional groups which may leads to the GO agglomerated structure. However, the anionic SDS surfactant interacts with GO layers through relatively weaker π-π interactions may not significantly reduce the agglomeration in GO structures [20]. Commonly, the graphite flakes exhibited a thicker flat surface consisting of many layers structure on the edges of GO layers which was clearly revealed that several graphitic layers were stacked together [21], as represented by the arrow in Fig. 2 (a). Meanwhile, a large crumpled layers structure was observed on the glass surface incorporated with GO dispersion, as shown in Fig. 2 (b). This type of agglomeration may be connected to the unbalanced of oriented graphite layer through an oxidation process [22].

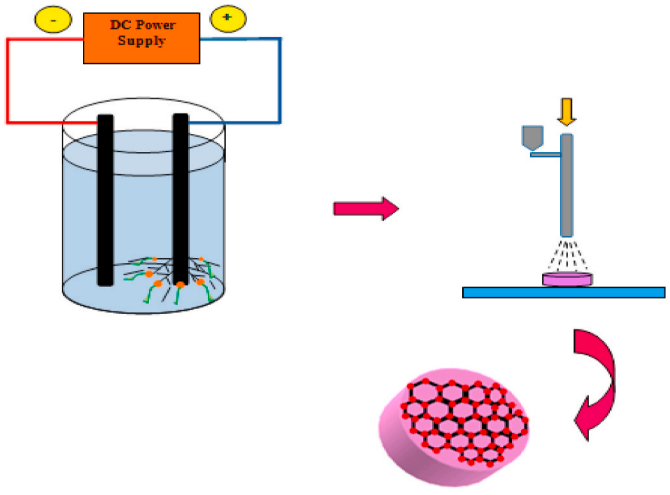

Fig. 1. Schematic diagrams for synthesis and deposition of GO onto tellurite-based glass surface.

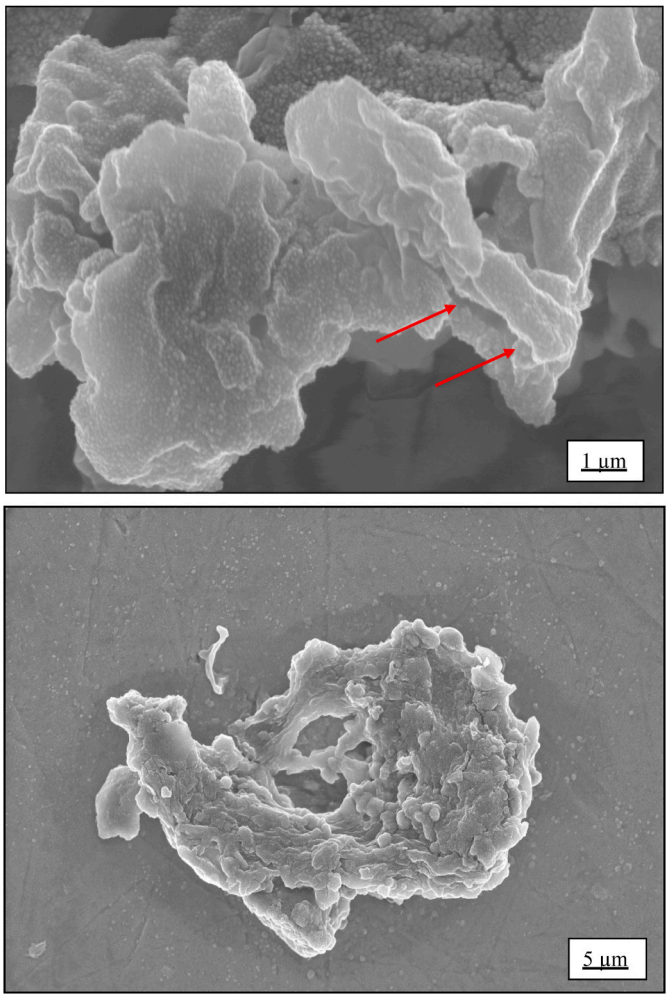

Fig. 2. The surface morphology of ZBTNd-GO glass surface with magnification at (a) 50 KX (b) 10 KX.

3.2. X-ray diffraction (XRD)

The XRD spectral measurement was analyzed of GO-coated tellurite glass doped with Nd^{3+}, as presented in Fig. 3. It can be observed that the spectral exhibited the broad diffusion at lower scattering angle at $2\theta = 30^{\circ}$ as having the continuous in pattern and also proved the structural arrangement of an amorphous in nature takes place in glass network system. Apparently, the prepared glass samples do not appear any discrete diffraction peaks on the diffraction spectrum which related to crystalline phases of any samples [23,24].

3.3. Optical absorption and optical coefficient

The study of optical absorption is important to determine the optical transitions in tellurite glass especially in terms of rare-earth transitions in glass matrix [25]. The transmission optical absorption along with wavelength of ZBTNd-GO glasses are illustrated in Fig. 4. It was shown from the figure that the absorption bands consist of several peaks in the glass system. The present of absorption bands are originated from ground state, $^4I_{9/2}$ to the excited states $^2P_{3/2}$, $^4G_{7/2}$, $^4G_{5/2}$, $^4F_{9/2}$, $^4F_{7/2}$, $^4F_{5/2}$, and $^4F_{3/2}$ which corresponds to the different excitation level. The absorption spectra possess several in-homogenously widened patterns due to *f-f* transitions in neodymium ions [26]. From the figure, it has been observed that the absorption coefficient increases along with wavelength which may be caused by the incorporation of GO itself as the coating material whereby the absorption of oxygenated functionality groups significantly influences the optical characteristics [27].

3.4. Optical bandgap, Urbach energy and refractive index

The absorption coefficient value was estimated according to the following relation:

$$\alpha\left(\omega\right) = 2.303\left(\frac{A}{d}\right) \tag{1}$$

where *d* represents the thickness of each glass samples and *A* is the absorbance value.

The indirect transition in band gap energy was estimated by relating absorption coefficient, α(ω) and photon energy through the following expression [28]:

$$\alpha\left(\omega\right) = \frac{\beta(\hbar\omega - Eopt)^n}{\hbar\omega} \tag{2}$$

β is band tailing parameter, E_{opt} is the optical bandgap energy, ħω is the photon energy, and *n* is a constant index which has values of ½ (direct transition), 2 (indirect transition), 3/2 (direct forbidden transition), and 3 (indirect forbidden transition) [29].

Fig. 5 refers the Tauc's plot to determine the optical bandgap energy. It has been found that the optical band gap energy can be calculated by extrapolating the curves and the obtained Results have been shown and tabulated in Fig. 5 and Table 1, respectively. From Fig. 6, it was found that the optical band gap energy displayed a non-linear trend along with neodymium oxide concentrations in the range of 3.253–3.381 eV. This trend can be associated with the shift in optical absorption due to the effect of GO layers. The comparison in the optical bandgap energy values between ZBTNd-GO and ZBTNd are presented in Fig. 6 and Table 1 [30].

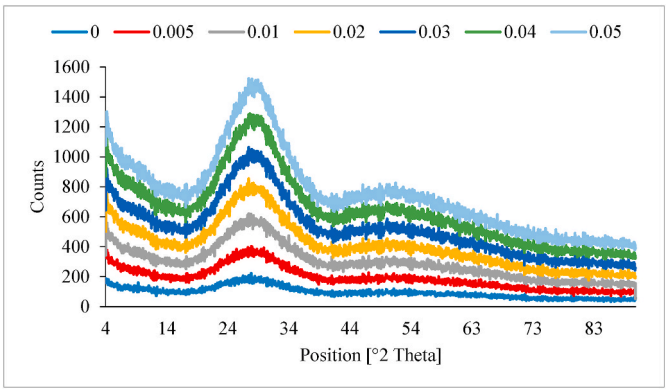

Fig. 3. XRD diffraction pattern of ZBTNd-GO glasses.

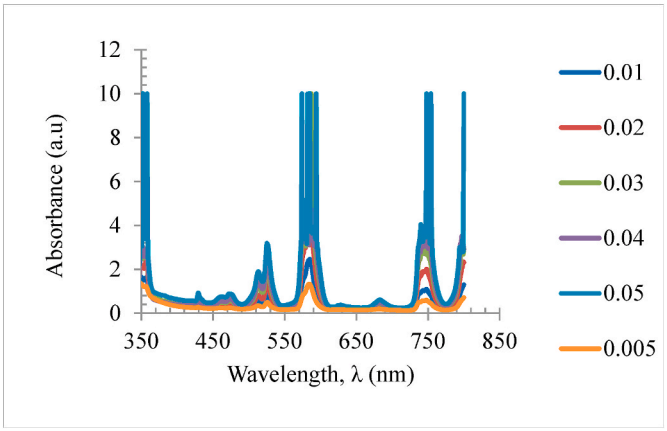

Fig. 4. Optical absorption spectra of ZBTNd-GO glasses.

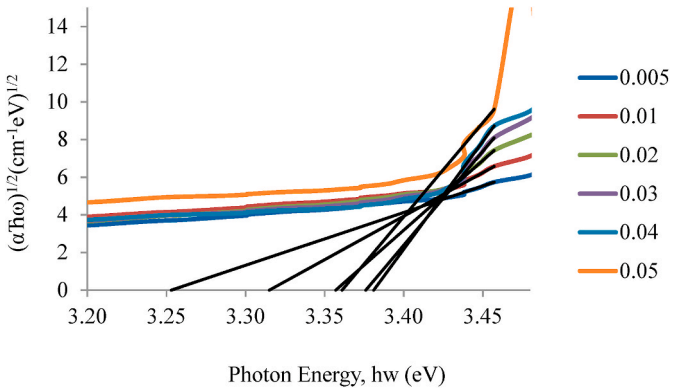

Fig. 5. Plot of $(\alpha\hbar\omega)^{1/2}$ against photon energy, $\hbar\omega$ of ZBTNd-GO glasses.

Table 1
Comparison of optical bandgap energy (E_{opt}) between ZBTNd and ZBTNd-GO glasses.

Nd molar fraction	ZBTNd	ZBTNd-GO
0.005	3.184 ± 0.1 nm [30]	3.253 ± 0.1 nm
0.01	3.183 ± 0.1 nm [30]	3.315 ± 0.1 nm
0.02	3.169 ± 0.1 nm [30]	3.357 ± 0.1 nm
0.03	3.163 ± 0.1 nm [30]	3.376 ± 0.1 nm
0.04	3.163 ± 0.1 nm [30]	3.381 ± 0.1 nm
0.05	3.151 ± 0.1 nm [30]	3.361 ± 0.1 nm

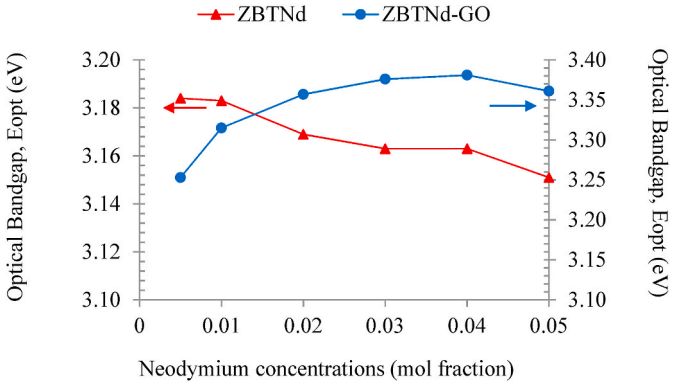

Fig. 6. Variation of optical bandgap values for ZBTNd and ZBTNd-GO glasses.

Fig. 6 depicts the variations of optical band gap energy for ZBTNd-GO glasses which is found higher than ZBTNd glasses. This result shows that the GO layers widen the forbidden gap of tellurite glass.

The surface modification of GO-containing oxygen is the core explanation to the widening of the forbidden gap between the valence and the conduction bands [31,32]. This trend may be correlated to the optical absorption in GO layers which are significantly affected by the effect of π and π* orbitals on the electronic transition during the oxidation process. The presence of π orbital has a lower energy than that of the π* orbital which indicates the photon-induced transition between these π and π* orbitals in the oxygen-containing functional groups [33,34]. Therefore, this transition incorporates an electron from a lone-pair non-bonding *n* orbital to the anti-bonding π* orbital through photon absorption [35]. In addition, the widening of the optical bandgap energy for ZBTNd-GO glasses was due to the strong optical absorption and the excess of oxygen content in the GO layers [36,37].

The Urbach energy, ΔE can be defined as a level of disorderness in glass materials [38]. The Urbach energy values can be calculated using the slope in lower photon energy and the plot of logarithm of absorption coefficient, In(α) versus photon energy, $\hbar\omega$ by the expressions:

$$\alpha\left(\omega\right) = \beta \exp\left(\frac{\hbar\omega}{\Delta E}\right) \tag{3}$$

This exponential behaviour shows that the band tails are associated with the valence and conduction bands [39]. The glass materials with high Urbach energy values have the tendency to convert the weak bonds into defects. Fig. 7 shows the variations of Urbach energy for ZBTNd-GO glasses and found in the range of 0.203–0.322 eV (see Table 2) [40]. The increasing trend in Urbach energy reflects to the growing number of defects in particular materials [41]. The Urbach energy values for ZBTNd-GO glasses were found higher than ZBTNd glasses which can be ascribed to the greater defects in GO layers. The GO layers consist with a large number of oxygens and large crumpled structure which contributes to high defects.

The refractive index n is a significant data to determine the capability of optoelectronics devices, especially in optical fiber and laser. Moreover, the refractive index is related to the interactions between the photon energy and electrons of the constituent atoms in solid materials. The refractive index values can be calculated using the following equation [42]:

$$\frac{n^2-1}{n^2+1} = 1 - \sqrt{\frac{Eopt}{20}} \tag{4}$$

where *n* is the refractive index and E_{opt} represents the optical bandgap energy. The plotted graph of refractive index for ZBTNd and ZBTNd-GO along with the neodymium oxide concentrations was depicted in Fig. 8. It can be seen from the figure that the refractive index, *n* values for ZBTNd-GO glasses exhibit an increasing pattern ranging from 2.301 to 2.332. Moreover, the refractive index for ZBTNd-GO glasses is found higher than ZBTNd glasses. This trend can be ascribed to the presence of high degree of oxygen and greater number of defects in GO layers. As can be referred in Table 3, it is noted that the GO layers improve the refractive index of tellurite glass.

On top of that, this improvement indicates that the GO layers have increased the optical properties of glass materials and are useful for fiber optics. High number in refractive index is beneficial for manufacturing the fiber core in optical fiber. Thus, it should be acknowledged that the inclusion of GO as the coating materials offers reasonable performance to be used in fiber core. In addition, the non-linear trend in refractive index for ZBTNd-GO glasses was attributed to the disparity in atomic and oxidation numbers in the GO layers [43,44].

3.5. *Electronic polarizability and oxide ion polarizability*

Electronic polarizability, α_e is the most important parameters that can be used to estimate the non-linear optical response to solid materials. Moreover, electronic polarizability can be expressed as a

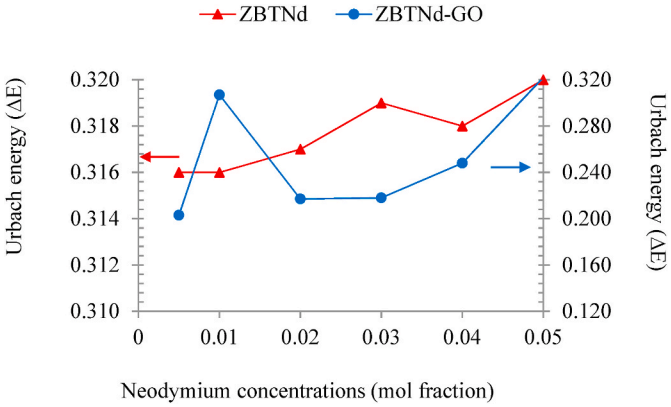

Fig. 7. Variation of Urbach energy for ZBTNd and ZBTNd-GO glasses.

Table 2
Comparison of Urbach energy (E_{opt}) between ZBTNd and ZBTNd-GO glasses.

Nd molar fraction	ZBTNd	ZBTNd-GO
0.005	0.316 ± 0.1 nm [40]	0.203 ± 0.1 nm
0.01	0.316 ± 0.1 nm [40]	0.307 ± 0.1 nm
0.02	0.317 ± 0.1 nm [40]	0.217 ± 0.1 nm
0.03	0.319 ± 0.1 nm [40]	0.218 ± 0.1 nm
0.04	0.318 ± 0.1 nm [40]	0.248 ± 0.1 nm
0.05	0.320 ± 0.1 nm [40]	0.322 ± 0.1 nm

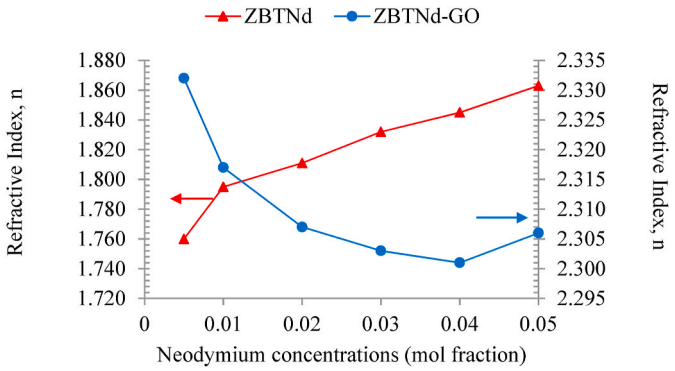

Fig. 8. Refractive index values for ZBTNd and ZBTNd-GO glasses.

Table 3
Comparison of refractive index, *n* between ZBTNd and ZBTNd-GO glasses.

Nd molar fraction	ZBTNd	ZBTNd-GO
0.005	1.760 ± 10 μm [40]	2.332 ± 10 μm
0.01	1.795 ± 10 μm [40]	2.317 ± 10 μm
0.02	1.811 ± 10 μm [40]	2.307 ± 10 μm
0.03	1.832 ± 10 μm [40]	2.303 ± 10 μm
0.04	1.845 ± 10 μm [40]	2.301 ± 10 μm
0.05	1.863 ± 10 μm [40]	2.306 ± 10 μm

magnitude of electron correlates to an electric field based on the following expression [45]:

$$\alpha_e = \left(\frac{3}{4\pi N_A}\right)\left(\frac{n^2-1}{n^2+2}\right) V_m \quad (5)$$

where N_A = Avogadro's number, n = refractive index, and V_m = molar volume in glass samples. As mentioned on the above equation, the refractive index depends on the type of oxides in glass materials which means the more polarizable of an outer electron, the higher the refractive index values, *n*. As noticed from Fig. 9, it can be seen that the electronic polarizability values of ZBTNd-GO glasses were found in the range of 8.815 Å^3 to 8.887 Å^3 which are greater than ZBTNd glasses [40].

The shift in electronic polarizability values for ZBTNd-GO glasses can be correlated to the high surface area and low particle density during the deposition process [46]. In addition, the high value of electronic polarizability reflects to the high number of refractive index and Te^{4+} ions existing in the glass system. Another explanation may have been the shift of polarization in GO layers under the total internal reflection (TIR) caused by the deposition of GO on the glass surfaces [47].

In particular, an estimation of oxide ion polarizability depends on the crystals and glasses, which may develop the technological importance as an optical and electronic materials [48]. The oxide ions can be defined as charge carriers in solid conductive materials and possessing the highly polarizable which often had been ignored in solid materials.

As a fact, the oxide ion polarizability possesses the increasing values resulted from oxygen contents which enable to be present not only as a bridging nor non-bridging but also in terms of a degree of negative charge, where it can be varied via modifying the glass composition [49]. The relationship between the $\sqrt{E_g}$ and $1-\frac{R_m}{V_m}$ for a higher number of the simple oxides as stated based on the following relation [50]:

$$E_g = 20\left(1-\frac{R_m}{V_m}\right)^2 \quad (6)$$

Therefore, the oxide ion polarizability can be calculated as indicated as the following relation:

$$\alpha_{O_2^-}(E_g) = \left[\frac{V_m}{2.52}\left(1-\sqrt{\frac{E_g}{20}}\right) - \sum \alpha_i\right]\left(N_{O_2^-}\right)^{-1} \quad (7)$$

where $\alpha_{O_2^-}(E_g)$refers to energy bandgap based on oxide ion polarizability, $\sum \alpha_i$ denotes as the molar fraction polarizability, and $N_{O_2^-}$ stand for number of oxide ions in chemical formula. Fig. 10 shows the plotted graph of oxide ion polarizability for ZBTNd and ZBTNd-GO glasses along with the glass system containing different Nd^{3+} ions molar fraction. It can be seen from the figure that the oxide ion polarizability values of ZBTNd-GO glasses lies in the range of 2.071 Å^3 to 3.467 Å^3 and for ZBTNd glasses are in the range of 3.359 Å^3 to 6.182 Å^3 [40], respectively as tabulated in Table 4.

It can be inferred that the addition of graphene-based materials on the glass coating caused the increment of energy gap in glass materials which contributed to the decreasing pattern in oxide ion polarizability. Additionally, the obtained oxide ion polarizability values can be related to an existence of localized states in bandgap energy by referring to David-Mott's theory for the conduction in a non-crystalline system [51]. Moreover, the type of bond between the oxygen and graphene gives major role to the oxide ion polarizability. It may be presumed that the bonding between oxygen and graphene is stronger than the bonding of oxygen in the glass network. Hence, the oxygens in graphene layers are unlikely to be more polarizable.

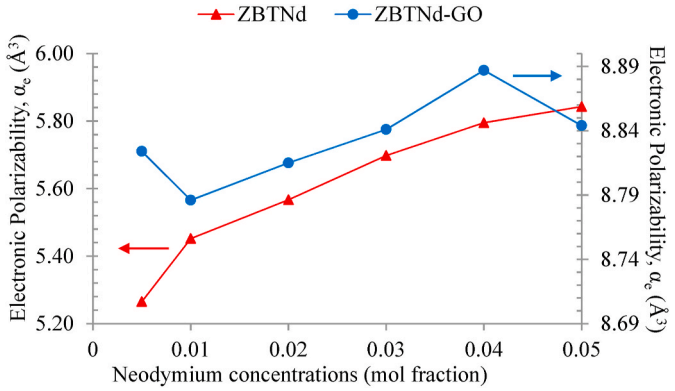

Fig. 9. Electronic polarizability values for ZBTNd and ZBTNd-GO glasses.

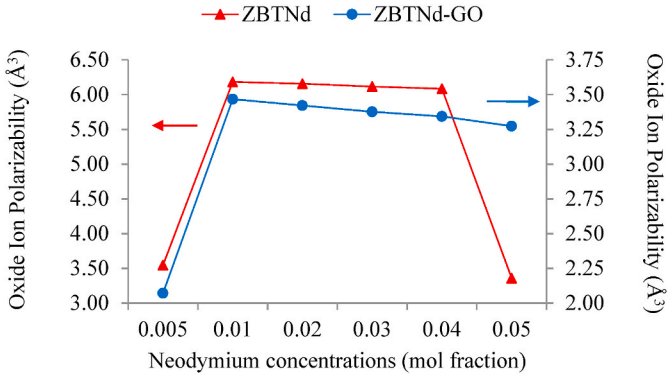

Fig. 10. Oxide ion polarizability values for ZBTNd and ZBTNd-GO glasses.

Table 4
Comparison of electronic polarizability and oxide ion polarizability values between ZBTNd and ZBTNd-GO glasses.

Nd molar fraction	Electronic polarizability, α_e (Å^3) (ZBTNd)	Electronic polarizability, α_e (Å^3) (ZBTNd-GO)	Oxide ion polarizability, $\alpha_{O_2^-}$ (Å^3) (ZBTNd)	Oxide ion polarizability, $\alpha_{O_2^-}$ (Å^3) (ZBTNd-GO)
0.005	5.265 [40]	8.824	3.546 [40]	2.071
0.01	5.452 [40]	8.786	6.182 [40]	3.467
0.02	5.567 [40]	8.815	6.156 [40]	3.421
0.03	5.698 [40]	8.841	6.115 [40]	3.376
0.04	5.795 [40]	8.887	6.084 [40]	3.343
0.05	5.843 [40]	8.844	3.359 [40]	3.273

3.6. Optical basicity and metallization criterion

Optical basicity is known as an electron donating material and a material containing oxide ions with high electron density is considered as high basicity [52]. Specifically, the optical basicity is related to solid chemical bonding through the polarizability of electron clouds surrounded by atoms or ions [53]. The theoretical calculation of optical basicity, Λ_{th} for any types of glasses can be obtained from the following expression suggested by Duffy and Ingram [50]:

$$\Lambda = X_1\Lambda_1 + X_2\Lambda_2 + \ldots\ldots + X_n\Lambda_n \quad (8)$$

where X_1, X_2, … …. , X_n represent the equivalent fractions of each oxides that attributes to an overall stoichiometry and Λ_1, Λ_2, … …, Λ_n denote as the optical basicity of each individual oxides in glass matrix. The optical basicity and oxide ion polarizability have been defined from the refractive index and energy gap for a glass system and can be calculated based on the relationship as follows [54]:

$$\Lambda = 1.67\left(1 - \frac{1}{\alpha_{O_2^-}}\right) \quad (9)$$

As displayed in Fig. 11, the plotted graph of an optical basicity for ZBTNd-GO glasses were found decreases slightly from 0.864 to 1.188 and for ZBTNd glasses are in the range of 1.173–1.401 [40], respectively with respect to the Nd^{3+} ions molar fraction. The comparison values of optical basicity between ZBTNd and ZBTNd-GO glasses are listed in Table 5. Decreasing values in optical basicity were influenced by the large number of oxygen-functionalized groups in GO surface layers and which can be seen to be less acidic in glass materials. The negative charge taken over by the oxygen atoms leads to a lower covalency of the cation-oxygen linking, which also significantly reduce the optical basicity in the glass system [55]. The incorporation of modifier oxide in former oxide resulted in a modification of the acid-base reaction where the acidity of former oxide has been reduced by modifier oxide [56].

Metallization criterion can be connected to the metallic or insulating nature of glass materials and demonstrates a propensity for materials to be more metallic [57,58]. As reported by Dimitrov and Komatsu, the metallic behaviour of glass materials can be defined as $\frac{R_m}{V_m} = 1$ or $\frac{R_m}{V_m} > 1$ whereas the non-metallic behaviour was estimated as $\frac{R_m}{V_m} < 1$, respectively [51]. The metallization criterion can be obtained by the following equation as stated below:

$$M = 1 - \frac{R_m}{V_m} \quad (10)$$

where R_m defines as the molar refraction and V_m refers to molar volume of glasses. The refractive index based on metallization criterion, M (n_0) can be calculated and expressed using the relation as follows:

$$M\left(n_0\right) = 1 - \left[\frac{n_0^2 - 1}{n_0^2 + 2}\right] \quad (11)$$

The metallization criterion values were calculated using Eq. (11) and presented in Table 5 with the comparative values between ZBTNd and ZBTNd-GO glasses. As observed from Fig. 12, the metallization criterion values for ZBTNd-GO glasses exhibit decreasing pattern in the range of 0.311–0.318 and for ZBTNd glasses lies in the range of 0.549–0.589 [40], respectively. The reduction in metallization criterion for ZBTNd-GO glasses can be related with the influence of GO layers that compromised a large amount of oxygenated functional groups which lead to an improvement of optical performance in glass materials. Moreover, graphene itself has zero band gap value which may reduce the forbidden gap of glass system. Hence, it can be justified that the existence of GO layers on the ZBTNd glass surface enhance the metallic properties of glass system and hence, improve the semiconductor properties [59].

Table 5
Comparison of optical basicity and metallization criterion values between ZBTNd and ZBTNd-GO glasses.

Nd molar fraction	Optical basicity, Λ (ZBTNd)	Optical basicity, Λ (ZBTNd-GO)	Metallization criterion (ZBTNd)	Metallization criterion (ZBTNd-GO)
0.005	1.401 [40]	0.864	0.589 [40]	0.311
0.01	1.400 [40]	1.188	0.574 [40]	0.314
0.02	1.399 [40]	1.182	0.568 [40]	0.316
0.03	1.397 [40]	1.175	0.560 [40]	0.317
0.04	1.396 [40]	1.170	0.555 [40]	0.318
0.05	1.173 [40]	1.159	0.549 [40]	0.316

4. Conclusion

In summary, the structural and optical properties of ZBTNd-GO glasses have been successfully investigated. The optical band gap and refractive index of ZBTNd-GO glasses values were shown to decrease

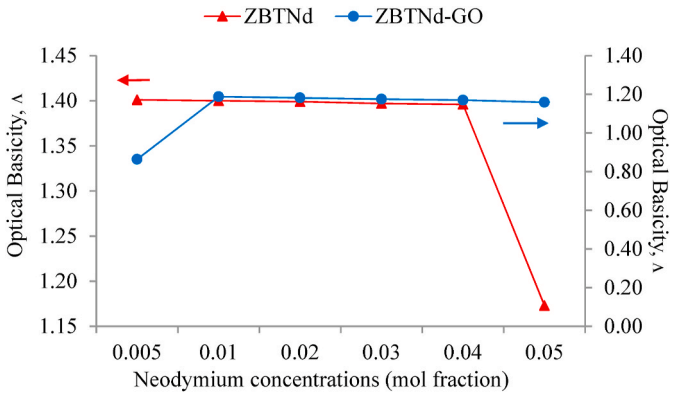

Fig. 11. Optical basicity values for ZBTNd and ZBTNd-GO glasses.

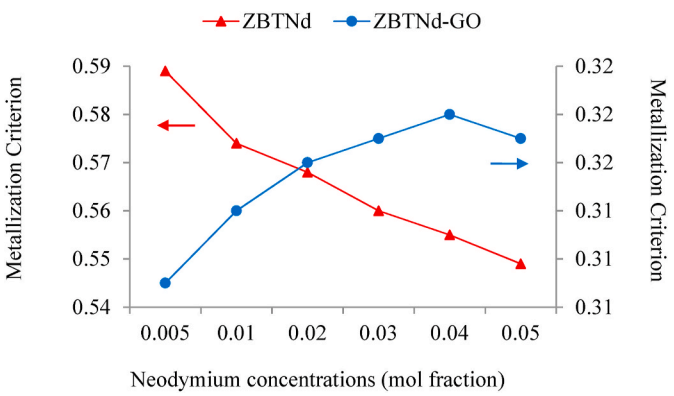

Fig. 12. Metallization criterion values for ZBTNd and ZBTNd-GO glasses.

along with neodymium oxide concentration. The morphological study revealed the existence of GO structure on glass surface while the XRD spectra proved that the prepared glasses are amorphous in nature. The refractive index of ZBTNd-GO glasses was found higher than ZBTNd glasses which was corresponded to the high concentrations of oxygens. The increasing number of optical band gap in ZBTNd-GO glasses than ZBTNd glasses may be due to the strong chemical bonding between oxygen and graphene. The oxide ion polarizability values were found to decrease which can be ascribed to the low polarizability of oxygen in graphene layers. The decreasing pattern found in metallization criterion explains that the ZBTNd-GO glasses tend to be more metallic. Therefore, by coating between tellurite glass and graphene oxide can be a new strategy to increase optical properties of tellurite glass system and this research is highly valuable to fiber optics applications.

Confirmation of authorship

As corresponding author, I Azlan M.N, hereby confirm on behalf of all authors that:

1 This manuscript has not been published, was not, and is not being submitted to any other journal. If presented at a conference, the conference is identified. If published in conference proceedings, substantial justification for republication must be presented.
2 All necessary permissions for publication were secured prior to submission of the manuscript.
3 All authors listed have made a significant contribution to the research reported and have read and approved the submitted manuscript, and furthermore, all those who made substantive contributions to this work have been included in the author list.

CRediT authorship contribution statement

Y. Azlina: Glass fabrication. **M.N. Azlan:** Supervision. **S.S. Hajer:** Formal analysis, UV–Vis characterization and analysis. **M.K. Halimah:** Formal analysis, XRD characterization and analysis. **A.B. Suriani:** Spray coating on glass. **S.A. Umar:** Formal analysis, FESEM characterization and analysis. **R. Hisam:** Data curation, Validation. **M.H.M. Zaid:** Formal analysis, Validation, Refractive index analysis and validation. **S. M. Iskandar:** Electronic polarizability calculation. **B.K. Kenzhaliyev:** Data curation, Validation, Optical basicity and metallization criterion data calculation and validation. **A.V. Nitsenko:** Validation, Materials validation and selection. **N.N. Yusof:** Graphene oxide synthesis. **Boukhris Imed:** Writing – review & editing.

Declaration of competing interest

The authors declare that they have no known competing financial interests or personal relationships that could have appeared to influence the work reported in this paper.

Acknowledgement

The authors extend their appreciation to the Deanship of Scientific Research at King Khalid University, Saudi Arabia for funding this work through Research Groups Program under grant number R.G.P.1/237/42. The authors would like to thank to Skim Geran Penyelidikan Fundamental (FRGS) Fasa 1/2018 (Grant code: 2019–0006–102–02), Kementrian Pengajian Tinggi, Malaysia for grant support.

References

[1] D.S. Shin, et al., Distribution of oxygen functional groups of graphene oxide obtained from low-temperature atomic layer deposition of titanium oxide, R. Soc. Chem. 7 (2017) 13979–13984.
[2] A.T. Smith, A. Marie, S. Zeng, B. Liu, L. Sun, Synthesis , properties , and applications of graphene oxide/reduced graphene oxide and their nanocomposites, Nano Mater. Sci. 1 (1) (2019) 31–47, https://doi.org/10.1016/j.nanoms.2019.02.004.
[3] J. Wang, X. Mu, M. Sun, T. Mu, Optoelectronic properties and applications of graphene-based hybrid nanomaterials and van der Waals heterostructures, Appl. Mater. Today 16 (2019) 1–20.
[4] I.K. Moon, J. Il Kim, H. Lee, K. Hur, W.C. Kim, H. Lee, 2D graphene oxide nanosheets as an adhesive over-coating layer for flexible transparent conductive electrodes, Sci. Rep. 3 (2013) 1–7.
[5] Z. Li, et al., Exceptional supercapacitor performance from optimized oxidation of graphene-oxide, Energy Storage Mater. 17 (2019) 12–21.
[6] T. Purkait, G. Singh, D. Kumar, M. Singh, R.S. Dey, High-performance flexible supercapacitors based on electrochemically tailored three-dimensional reduced graphene oxide networks, Sci. Rep. 8 (640) (2018) 1–13.
[7] Q. Cheng, Y. Okamoto, N. Tamura, M. Tsuji, S. Maruyama, Graphene-like-graphite as fast- chargeable and high-capacity anode materials for lithium ion batteries, Sci. Rep. 7 (14782) (2017) 1–14.
[8] S. Augustine, J. Singh, M. Srivastava, M. Sharma, A. Das, B.D. Malhotra, Biomaterials Science Recent advances in carbon based nanosystems for cancer theranostics, Biomater. Sci. 5 (2017) 901–952.
[9] M. Czerniak-Reczulska, A. Niedzielska, A. Jędrzejczak, Graphene as a material for solar cells applications,, Adv. Mater. Sci. 15 (4) (2015) 46.
[10] A. Nourbakhsh, et al., Bandgap opening in oxygen plasma-treated graphene, Nanotechnology 21 (43) (2010), 435203.
[11] V. Gupta, N. Sharma, U. Singh, M. Arif, A. Singh, (Revised Manuscript) Synthesis and Characterization of Graphene Oxide, *Optik (Stuttg).*, 2017.
[12] S.Y. Gu, C. Te Hsieh, T.W. Lin, J.K. Chang, J. Li, Y.A. Gandomi, Tuning oxidation level, electrical conductance and band gap structure on graphene sheets by a cyclic atomic layer reduction technique, Carbon N. Y. 137 (2018) 234–241.
[13] A.G. Kalampounias, N.K. Nasikas, G.N. Papatheodorou, "Journal of Physics and Chemistry of Solids tellurite glasses : a composition dependent Raman spectroscopic study, J. Phys. Chem. Solid. 72 (9) (2011) 1052–1056.
[14] C. Yu, et al., Photoluminescence properties of tellurite glasses doped Dy^{3+} and Eu^{3+} for the UV and blue converted WLEDs, J. Non-Cryst. Solids 457 (2017) 1–8.
[15] L. Hu, et al., Research and development of neodymium phosphate laser glass for high power laser application, Opt. Mater. (Amst). 62 (2016) 34–41.
[16] K. Nasser, V. Aseev, S. Ivanov, A. Ignatiev, N. Nikonorov, "Optical, spectroscopic properties and Judd–Ofelt analysis of Nd^{3+}-doped, J. Lumin. 213 (2019) 255–262.
[17] M. Shoaib, N. Chanthima, G. Rooh, N. Sangwaranatee, J. Kaewkhao, Physical and luminescence study of Nd^{3+} ions doped phosphate glass for lasing applications, Mater. Today Proc. 17 (2019) 1800–1808.
[18] R. Narayan, S.O. Kim, Surfactant mediated liquid phase exfoliation of graphene, Nano Converg. 2 (1) (2015) 20.
[19] R.J. Smith, M. Lotya, J.N. Coleman, The importance of repulsive potential barriers for the dispersion of graphene using surfactants, New J. Phys. 12 (2010), 125008.
[20] X. Cai, et al., Surfactant-assisted synthesis of reduced graphene oxide/polyaniline composites by gamma irradiation for supercapacitors, J. Mater. Sci. 49 (16) (2014) 5667–5675.
[21] P.B. Arthi G, L. Bd, A simple approach to stepwise synthesis of graphene oxide nanomaterial, J. Nanomed. Nanotechnol. 6 (1) (2015), 1000253.
[22] H. Saleem, M. Haneef, H.Y. Abbasi, Synthesis route of reduced graphene oxide via thermal reduction of chemically exfoliated graphene oxide, Mater. Chem. Phys. 204 (2018) 1–7.
[23] M.R. Dousti, R.J. Amjad, Enhanced 1.06 μm emission in Nd^{3+}-doped lead-tellurite glasses doped with silver nanoparticles, J. Nanophotonics 10 (4) (2017), 046010.
[24] G. Lakshminarayana, I. V Kityk, M.A. Mahdi, K.J. Plucinski, Er/Pr-codoped borotellurite glasses as efficient laser operated nonlinear optical materials, Mater. Lett. 214 (2017) 23–25.
[25] M.F. Faznny, M.K. Halimah, M.N. Azlan, Effect of lanthanum oxide on optical properties of zinc borotellurite glass system, J. Optoelectron. Biomed. Mater. 8 (2) (2016) 49–59.
[26] K. Anita, N.R. Singh, "Spectrochimica Acta Part A : molecular and Biomolecular Spectroscopy Absorption spectral analysis of 4f–4f transitions for the complexation of Pr(III) and Nd(III) with thiosemicarbazide in absence and presence of Zn(II) in aqueous and organic solvents, Spectrochim. Acta Part A Mol. Biomol. Spectrosc. 81 (1) (2011) 117–121.
[27] T. Hasan, et al., Optical band gap alteration of graphene oxide via ozone treatment, Sci. Rep. 7 (1) (2017).
[28] N.F. Mott, E.A. Davis, K. Weiser, Electronic processes in non-crystalline materials, Phys. Today 25 (12) (1972) 14–15.
[29] W. Stambouli, H. Elhouichet, M. Ferid, Study of thermal, structural and optical properties of tellurite glass with different TiO_2 composition, J. Mol. Struct. 1028 (2012) 39–43.
[30] M.N. Azlan, M.K. Halimah, S.O. Baki, W.M. Daud, Effect of neodymium concentration on structural and optical properties of tellurite based glass system, Mater. Sci. Forum 846 (2016) 183–188.
[31] G. Eda, C. Mattevi, H. Yamaguchi, H. Kim, M. Chhowalla, Insulator to semimetal transition in graphene oxide, J. Phys. Chem. C 113 (35) (2009) 15768–15771.
[32] S. Li, Ḱ.K. Tu, Ḱ.C. Lin, C. Chen, M. Chhowalla, Solution-processable graphene oxide as an efficient hole transport layer in polymer solar cells, ACS Nano 4 (6) (2010) 3169–3174.
[33] J. Shang, J. Li, W. Ai, T. Yu, G.G. Gurzadyan, The origin of fluorescence from graphene oxide, Sci. Rep. 2 (1) (2012) 1–8.
[34] X. Zhang, X. Shao, S. Liu, Dual fluorescence of graphene oxide: a time-resolved study, J. Phys. Chem. A 116 (27) (2012) 7308–7313.
[35] A. V Naumov, Graphene Oxide: Fundamentals and Applications, *John Wiley Sons*, 2017.

[36] S. Tang, W. Wu, X. Xie, X. Li, J. Gu, Band gap opening of bilayer graphene by graphene oxide support doping, R. Soc. Chem. 7 (2017) 9862–9871.
[37] Q. Lai, S. Zhu, X. Luo, M. Zou, S. Huang, Ultraviolet-visible spectroscopy of graphene oxides, AIP Adv. 2 (3) (2012) 3–8.
[38] J.N. Ayuni, et al., Optical properties of ternary TeO_2-B_2O_3-ZnO glass system, IOP Conf. Ser. Mater. Sci. Eng. 17 (2011), 012027.
[39] V. Dimitrov, S. Sakka, Linear and nonlinear optical properties of simple oxides. II, J. Appl. Phys. 79 (3) (1996) 1741–1745.
[40] M.N. Azlan, M.K. Halimah, A.B. Suriani, Y. Azlina, R. El-Mallawany, Electronic polarizability and third-order nonlinearity of Nd^{3+} doped borotellurite glass for potential optical fiber, Mater. Chem. Phys. 236 (2019).
[41] Z.A. Said Mahraz, M.R. Sahar, S.K. Ghoshal, M. Reza Dousti, Concentration dependent luminescence quenching of Er^{3+}-doped zinc boro-tellurite glass, J. Lumin. 144 (2013) 139–145.
[42] V. Dimitrov, T. Komatsu, Electronic polarizability, optical basicity and non-linear optical properties of oxide glasses, J. Non-Cryst. Solids 249 (1999) 160–179.
[43] L. Ding, C. Xu, Z. Xia, B. Xu, J. Huang, Controlling polarization-dependent optical absorption of graphene through its thickness, Opt. Int. J. Light Electron Opt. 137 (2017) 59–64.
[44] I.A.E. Elbadawi, M.D. Abdallah, R.A. Elhai, S.A.E. Ahmed, The effect of oxidation number on refractive index based on string theory, Int. J. Eng. Sci. Res. Technol. 7 (1) (2018) 122–129.
[45] E. Talebian, M. Talebian, "A general review on the derivation of Clausius – mossotti relation, Opt. Int. J. Light Electron Opt. 124 (16) (2013) 2324–2326.
[46] W.L. Zhang, H.J. Choi, "Graphene/graphene oxide : a new material for electrorheological and magnetorheological applications, J. Intell. Mater. Syst. Struct. 26 (14) (2015) 1826–1835.
[47] C. Guo, et al., Graphene-based perfect absorption structures in the visible to terahertz band and their optoelectronics applications, Nanomaterials 8 (12) (2018) 1033.
[48] X. Zhao, X. Wang, H. Lin, Z. Wang, Electronic polarizability and optical basicity of lanthanide oxides, Phys. B 392 (2007) 132–136.
[49] J. Qi, D. Xue, H. Ratajczak, G. Ning, Electronic polarizability of the oxide ion and density of binary silicate , borate and phosphate oxide glasses, Phys. B 349 (2004) 265–269.
[50] M.D. Duffy, J. A, Ingram, Establishment of an optical scale for lewis basicity in inorganic oxyacids, molten salts, and glasses 1 (2) (1971) 6448–6454.
[51] V. Dimitrov, T. Komatsu, "Classification of oxide glasses : a polarizability approach, J. Solid State Chem. 178 (3) (2005) 831–846.
[52] T. Nanba, Characterization of glasses based on basicity, J. Ceram. Soc. Jpn. 119 (10) (2011) 720–725.
[53] V. Dimitrov, T. Komatsu, An interpretation of optical properties of oxides and oxide glasses in terms of the electronic ion polarizability and average single bond strength, J. Univ. Chem. Technol. Metall. 45 (3) (2010) 219–250 (review).
[54] V. Dimitrov, S. Sakka, Electronic oxide polarizability and optical basicity of simple oxides, J. Appl. Phys. 79 (3) (1996) 1736–1740.
[55] B. Bhatia, S.L. Meena, V. Parihar, M. Poonia, Optical basicity and polarizability of Nd^{3+}-doped bismuth borate glasses, New J. Glass Ceram. 5 (2015) 44–52.
[56] A.A. Sidek, S.P. Chow, Z.A. Talib, Formation and elastic behavior of lead-magnesium chlorophosphate glasses, Turk. J. Phys. 28 (2004) 65–71.
[57] S.H. Alazoumi, et al., Optical properties of zinc lead tellurite glasses, Results Phys. 9 (2018) 1371–1376.
[58] M.K. Halimah, M.F. Faznny, M.N. Azlan, H.A.A. Sidek, Optical basicity and electronic polarizability of zinc borotellurite glass doped La^{3+} ions, Results Phys. 7 (2017) 581–589.
[59] K.F. Herzfeld, On atomic properties which make an element a metal, Phys. Rev. 29 (1927) 701–705.